JOURNAL OF SOLID STATE CHEMISTRY 71, 109–114 (1987)

Spectroscopic Properties of Trivalent Chromium in the Fluoride Garnet $Na_3In_2Li_3F_{12}$

D. DE VIRY,* J. P. DENIS, AND B. BLANZAT

E.R. 211 du CNRS, École Centrale, Grande voie des Vignes, 92290 Chatenay Malabry, France

AND J. GRANNEC

Laboratoire de Chimie du Solide, 351 cours de la Libération, 33405 Talence, France

Received October 20, 1986; in revised form January 21, 1987

The spectroscopic properties of the fluoride garnet $Na_3In_2Li_3F_{12}:Cr^{3+}$, relevant for tunable laser emission, are investigated. In view of the excitation spectrum, the $^4T_2$ band can be assigned at 630 nm and the $^4T_1$ band at 436 nm. The emission spectrum, corresponding to the $^4T_2$–$^4A_2$ transition, is centered at 770 nm at 300 K with a bandwidth of 130 nm. The Tanabe–Sugano parameter Dq/B is 2.1. The $^4T_2$ level lifetime is long even at 300 K (320 μsec). These properties favor the chromium-doped fluoride garnet as a promising material for a room-temperature, tunable, and Q-switchable laser.

Introduction

Since the discovery of alexandrite (*1*), chromium-doped vibronic lasers have been developed during the last few years. Although oxide garnet crystals have been widely investigated as laser hosts (*2, 3*), fluoride compounds seem to attract more and more attention. A few oxide materials are low-field matrices, and this condition is fulfilled only when heavy ions, such as rare earths in gallate garnets, are used. On the contrary, the higher electronegativity of fluorine leads to an easier elaboration of chromium-doped host matrices with a low crystalline field, a necessary condition to obtain a broad band for chromium fluorescence. This is reflected in the large variety of fluorine materials displaying this property (*4*).

There are two sets of possibilities when choosing a laser material. They are determined by the relation

$$\tau = \lambda^2/8\pi c n^2 \Delta v \sigma_L,$$

where τ is the Cr^{3+} fluorescence lifetime, Δv is the emission bandwidth, σ_L is the stimulated emission cross section, and n is the refractive index, which is generally lower in fluorides than in oxides, allowing τ to be higher while σ_L remains constant.

The first possibility is to work in the Q-switch laser mode, where high-intensity pulses are delivered. In this case, the emission lifetime must be long enough to ensure a good energy storage in the laser level. If, however, a low laser threshold is desired,

* To whom all correspondence should be addressed.

0022-4596/87 $3.00

τ_L must be high and consequently τ is short.

The lifetime of Cr^{3+} in the fluorides investigated can vary from a few tens of microseconds ($SrGaF_5$) to hundreds of microseconds (K_2LiGaF_6) (*5*), depending on the distortion of the substitution site and on the energy difference between the ^2E and $^4T_2$ levels.

To enlarge the existing range of fluoride compounds, we focus our interest on indium compounds with In^{3+} in the octahedral site for the Cr^{3+} substitution. Since the strength of the crystalline field decreases with the Cr–F distance, it is interesting to use a large ion in the octahedral site to obtain a large site for the Cr^{3+} (r = 0.75 Å). This fact favors In^{3+} (r = 0.93 Å) compared to Ga^{3+} (r = 0.76 Å) or Al^{3+} (r = 0.67 Å).

In the series of fluoride garnets with indium in an octahedral site, only $Na_3In_2Li_3F_{12}$ has been obtained, as powder, by de Pape *et al.* (*6*). Doping with Cr^{3+} is easy in this structure because this ion totally substitutes into the octahedral site, leading to the isostructural garnet $Na_3Cr_2Li_3F_{12}$. Furthermore, we expect that the large number |98| of lattice vibrations (*7*) provided by the garnet structure (160 atoms per unit cell) will enhance vibronic emission.

Synthesis

The indium garnet $Na_3In_2Li_3F_{12}$ has been synthesized at 550°C under fluorine flow. The starting materials were mixed in stoichiometric proportions and the reaction occurring in an alumina boat was

$$3NaF + 3LiF + In_2O_3 \rightarrow Na_3In_2Li_3F_{12} + \tfrac{3}{2}O_2.$$

The powder obtained was white.

The compound $Na_3Cr_2Li_3F_{12}$ was prepared directly with the fluorides LiF, NaF, and CrF_3 as starting materials. They were placed in a platinum tube sealed under dry argon atmosphere. The temperature of the reaction was 600°C during 15 hr. The doped material (1% Cr^{3+}) was obtained by solid-state reaction between the two garnets in a platinum tube heated at 600°C for 40 hr. The powder obtained was green.

The crystal is cubic, with space group $Ia3d$, lattice parameter a = 12.7 Å, Z = 8, and density d = 3.54 g/cm^3 (*6*).

Experimental

Fluorescence spectra were recorded using the 458-nm line of an argon laser as a source and either a Jarrell-Ash spectrometer equipped with an S_1 (RCA 7102) photomultiplier or a Jobin Yvon HR 1000 spectrometer equipped with an S_{20} (Hamamatsu R649) photomultiplier.

The temperature was lowered down to 10 K using a CTI Cryogenics LTS 21 cooler.

Excitation spectra were obtained by measuring the intensity of fluorescence emission at a fixed wavelength and varying the excitation wavelength using a tungsten halogen lamp coupled to a motorized monochromator. The IR spectra were recorded on a Perkin–Elmer spectrophotometer.

For lifetime measurements, excitation flashes are generated by a Strobotac General Radio flash lamp. The wavelength (4295 Å) was selected by a M25 Jobin Yvon monochromator. The signal detected with an RTC 56 TVP photomultiplier was fed via a 164 PAR preamplificator to a PAR 162 boxcar integrator and the output displayed via an X-Y recorder.

Results

Crystalline Field

The band positions have been assigned using fluorescence and excitation spectra at 300 K (Fig. 1). Following the analysis of Kenyon *et al.* (*8*) for $K_2NaScF_6:Cr^{3+}$, we assigned the first broad band at 630 nm in

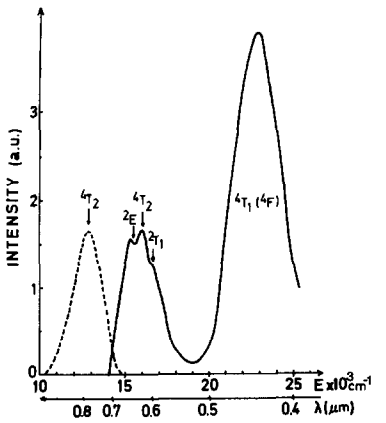

FIG. 1. Emission (dashed line) and excitation (solid line) spectra of Cr^{3+} in $Na_3In_2Li_3F_{12}$ at 300 K.

the excitation spectrum to the $^4T_2 \rightarrow {}^4A_2$ transition, because of its mirror symmetry with the fluorescence band. The 436-nm broad band corresponds to the $^4A_2 \rightarrow {}^4T_1(^4F)$ transition.

The features on the $^4T_2$ band are generally interpreted as Fano resonances (*9*). In our case, this was confirmed by the fact that their positions remain constant with decreasing temperature. The "notch" at 645 nm is assigned to the interaction of the ^2E level with the $^4T_2$ band, and the shoulder at 610 nm to that of the $^2T_1$ level.

Indeed, these features give only a rough approximation of their energy. For comparison, the ^2E level in the strong field of $K_2NaAlF_6:Cr^{3+}$ is at 15,045 cm^{-1} (664.7 nm). However, at least the "notch" position seems to be nearly the same in most of the low-field fluorides (*4, 5*) and we used it for the ^2E position in the crystalline field calculations. The emission band is centered at 770 nm and is 130 nm wide. The emission–absorption band overlap is small. The fluorescence is purely $^4T_2$ since the emission band does not extend to the ^2E-level region.

We followed the procedure of Struve and Huber (*2*) to determine the crystalline field parameters. Dq is taken from the maximum of the excitation band (Dq = 1587 cm^{-1}) and B is given by diagonalizing the Tanabe–Sugano matrices for $^4T_1(^4P)$ and $^4T_1(^4F)$ states.

Finally,

$$10 \cdot Dq = E_a(^4T_2) - E(^4A_2) \quad (1)$$

$$E_a(^4T_1) - E_a(^4T_2) = Dq \cdot x \quad (2)$$

$$15 \cdot B = Dq \cdot x \cdot (x - 10)/(x - 8), \quad (3)$$

where E_a is the energy at the absorption maximum of the band and x is defined by Eq. (2). Then B = 734 cm^{-1} and Dq/B = 2.1. The C parameter is determined by fitting the calculated ^2E energy level to the notch of the $^4T_2$ band. In this case C = 3390 cm^{-1}, C/B = 4.6. Using these parameters, the other levels are calculated to be

$^2T_1$: 16,174 cm^{-1} (618 nm)

$^2T_2$: 22,974 cm^{-1} (435 nm)

$^4T_1(^4F)$: 22,919 cm^{-1} (436 nm)

$^4T_1(^4P)$: 35,701 cm^{-1} (280 nm)

Low-Temperature Spectra

Emission and excitation spectra at low temperature (10 K) are shown in Figs. 2 and 3. The zero phonon line is located ay 697

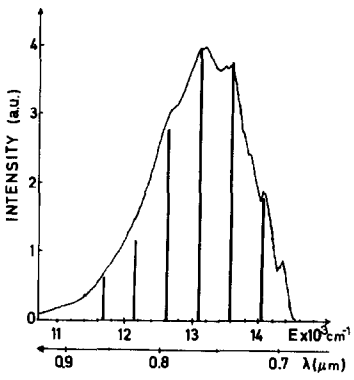

FIG. 2. Low-temperature $^4T_2 \rightarrow {}^4A_2$ emission spectrum of $Na_3In_2Li_3F_{12}:Cr^{3+}$ at 10 K. The zero phonon line is at 14,347 cm^{-1}, resolution is 15 cm^{-1}, and λ_{exc} = 0.458 μm.

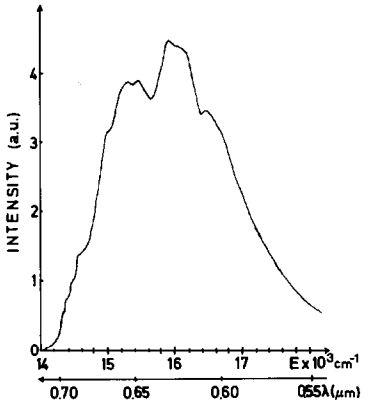

FIG. 3. Low-temperature excitation spectrum of $Na_3In_2Li_3F_{12}:Cr^{3+}$ at 10 K. The resolution is 40 cm^{-1}.

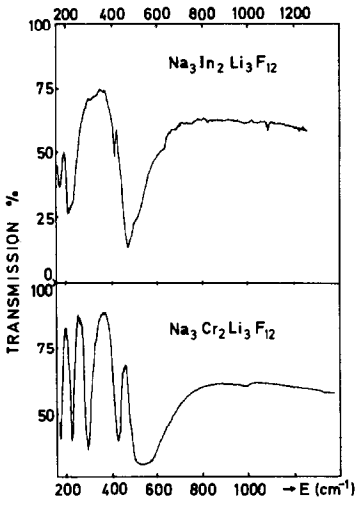

FIG. 5. Infrared spectra of $Na_3In_2Li_3F_{12}$ and $Na_3Cr_2Li_3F_{12}$ at 300 K.

nm (14,347 cm^{-1}) and corresponds to the magnetic dipolar allowed transition $^4T_2 \rightarrow {}^4A_2$.

There is no evidence for an ^2E line emission in the spectrum.

The emission spectrum exhibits a rich vibronic structure (Fig. 4), its main feature being due to the $(CrF_6)^{3-}$ octahedron local vibrations. These vibrations have been identified by comparison with compounds showing similar octahedral Cr^{3+} surroundings (*10*).

In order to make an accurate assessment of the energy of the antisymmetric t_{1u} vibrations, the IR spectra of pure indium garnet and pure chromium ($Na_3Cr_2Li_3F_{12}$) garnet were recorded (Fig. 5). Comparison between the two makes it possible to distinguish between vibrations due to chromium octahedra and to matrix vibrations.

The position of the lines and the vibrational analysis are given in Table I.

The first line due to $(CrF_6)^{3-}$ vibrations are t_{2u} (220 cm^{-1}) and t_{1u} (300 cm^{-1}), which

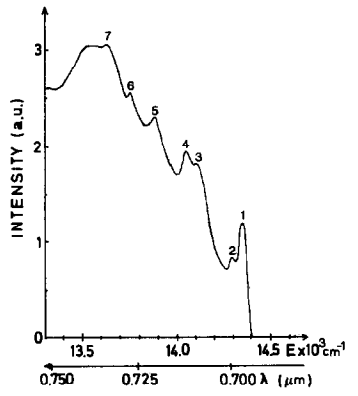

FIG. 4. Low-temperature $^4T_2 \rightarrow {}^4A_2$ emission spectrum of $Na_3In_2Li_3F_{12}:Cr^{3+}$ near the zero phonon (1) line, at 10 K. The positions of the lines are given in Table I.

TABLE I

ENERGY OF THE FIRST VIBRATIONS ASSOCIATED TO THE $^4T_2$–$^4A_2$ TRANSITION IN $Na_3In_2Li_3F_{12}:Cr^{3+}$

Line	Energy (cm^{-1})[a,b]	Assignment
1	0	Zero phonon
2	60	Lattice
3	220	t_{2u}
4	300	t_{1u}
5	470	e_g
6	600	a_{1g}
7	720	$e_g + t_{2u}$

[a] Energy difference with the zero phonon line at 14,347 cm^{-1}.

[b] ± 10 cm^{-1}.

allow dipolar electric transition of T_{1u} symmetry to occur:

$$^4T_{2g} \xrightarrow{D \cdot E} \left.\begin{matrix} t_{1u} \\ t_{2u} \end{matrix}\right\} + A_{2g}.$$

In the region of the assigned t_{2u} vibration, there is a peak in the IR spectrum of pure indium garnet corresponding to a $t_{1u}(InF_6)^{3-}$ vibration (226 cm^{-1}) (*11*). There is also a peak at 220 cm^{-1} in the chromium garnet spectrum. In this region the Cr^{3+} octahedron t_{2u} vibration can be resonant with lattice modes.

The t_{1u} vibration is assigned unambiguously from comparison of the fluorescence and the IR spectra, this line being present only in the chromium IR spectrum.

Regarding the symmetric modes, the lines at 470 and 600 cm^{-1} in the fluorescence spectrum are attributed to e_g and a_{1g} modes, respectively. The remaining progression is based on $t_{2u} + n \cdot e_g + m \cdot a_{1g}$ and $t_{1u} + n \cdot e_g + m \cdot a_{1g}$.

It is difficult to assign each term accurately because $a_{1g} + t_{2u}$ and $e_g + t_{1u}$ are very close. For lower energies, however, the energy difference between the remaining features is nearer to e_g than to a_{1g}, and this favors a dominant e_g mode for the building of the spectrum.

In this case, the intensity distribution in the spectrum is fitted by a Pekarian curve (*9, 12*) (Fig. 2),

$$I_n = I_0 \cdot e^{-S} \cdot S^n/n!,$$

where I_n is the intensity of the line corresponding to the nth e_g vibration, I_0 is the intensity corresponding to the false origin (t_{2u}, t_{1u}), and S is the Huang Rhys factor. The value of S is 2.1 in the present case, which implies a relatively low e_g vibration coupling for a transition metal compound (*8*).

Lifetime Measurements

The $^4T_2$-level fluorescence lifetime decreases with temperature as shown in Fig. 6. The decay curves were exponential at all temperatures.

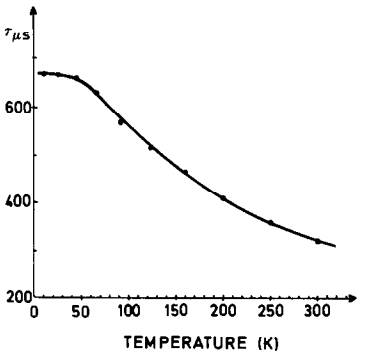

FIG. 6. Temperature dependence of the fluorescence lifetime for $Na_3In_{1.98}Cr_{0.02}Li_3F_{12}$. Excitation = 0.423 μm; analysis >0.670 μm.

Up to 300 K, this decrease can be fitted by

$$\frac{1}{\tau} = \frac{1}{\tau_0} + s_{exp}(E/kT),$$

where $\tau_0 = 672$ μsec is the extrapolated lifetime at $T = 0$ K, which is supposed to be equal to the lifetime at $T = 10$ K as it remains constant until $T = 50$ K, $s = 4.8 \times 10^3$ sec^{-1}, and $E = 218$ cm^{-1}. This decrease is too slow to correspond to a nonradiative de-excitation process, because the activation energy would be many times higher (*13*).

In the case of alexandrite, the temperature dependence of the lifetime is dominated by the interaction between the $^4T_2$ band and the ^2E line and follows the law

$$\frac{1}{\tau} = \frac{\dfrac{1}{\tau(^2E)} + \dfrac{3}{\tau(^4T_2)} e^{-\Delta/kT}}{1 + 3e^{-\Delta/kT}},$$

where τ is the measured lifetime, $\tau(^2E)$ and $\tau(^4T_2)$ are the intrinsic lifetimes of the levels measured at $T = 0$ K, and Δ is the positive energy difference between the $^4T_2$ and the ^2E zero phonon levels.

In our compound Δ is negative and if the long-lived ^2E level alone was to contribute, the lifetime should increase with tempera-

ture. This is obviously not the case. As $\Delta \simeq 1000\ cm^{-1}$, the ^2E level should not even lengthen the lifetime at 300 K. Since the E energy is of the same order of magnitude as that of the antisymmetric vibrations, we can assume that the lifetime dependence is simply due to stronger phonon coupling with temperature (*2, 14*).

It is interesting to note that at low temperature, the lifetime of the $^4T_2$ level is relatively long (672 μsec). This cannot be explained by a mixing with the ^2E level via spin–orbit coupling (*2*), because the energy difference is high compared to the spin–orbit parameter, $V_{so} = 170\ cm^{-1}$ (*15*). However, this lifetime is comparable to that measured in another compound (K_2NaScF_6 (*1*)) in which the chromium site is also centrosymmetric. On the contrary, in fluorides where the chromium emission is short-lived, this fact can be explained by distortion of their octahedral sites (*5*). This long lifetime should simply reflect the forbiddenness of the transition.

In conclusion, the promising optical properties, such as long and purely radiative lifetime, should make this fluoride garnet suitable for tunable, Q-switch laser application.

References

1. J. C. Walling, O. G. Peterson, H. P. Jenssen, R. C. Morris, and E. W. O'Dell, *IEEE J. Quantum Electron.* **16,** 1302 (1980).
2. B. Struve and G. Huber, *Appl. Phys. B* **36,** 195 (1985).
3. W. A. Wall, J. T. Karpick, and B. di Bartolo, *J. Phys. C* **4,** 3259 (1971).
4. U. Brauch and U. Dürr, *Opt. Lett.* **9,** 441 (1984).
5. W. F. Krupke, *in* "Tunable Solid State Lasers for Remote Sensing," Springer Series in Optical Sciences, Springer-Verlag, New York/Berlin.
6. R. de Pape, J. Portier, J. Grannec, G. Gauthier, and P. Hagenmuller, *C.R. Acad. Sci. Paris Sér. C* **269,** 1121 (1969); R. de Pape, J. Portier, G. Gauthier, and P. Hagenmuller, *C.R. Acad. Sci. Paris Sér. C* **265,** 1244 (1967).
7. N. T. McDevitt, *J. Opt. Soc. Amer.* **59,** 1240, (1969).
8. P. T. Kenyon, L. Andrews, B. McCollum, and A. Lempicki, *IEEE J. Quantum Electron.* **18,** 1189 (1982).
9. M. D. Sturge, H. J. Guggenheim, and M. H. L. Pryce, *Phys. Rev. B* **2,** 2459 (1970); A. Lempicki, L. Andrews, S. J. Nettel, B. C. McCollum, and E. I. Solomon, *Phys. Rev. Lett.* **44,** 1234 (1980).
10. P. Greenough and A. G. Paulusz, *J. Chem. Phys.* **70,** 1967 (1979); L. Dubicki, J. Ferguson, and B. van Oosterhout, *J. Phys. C* **13,** 2791 (1980).
11. K. Nakamoto, "Infrared Spectra of Inorganic and Coordination Compounds," 3rd ed., Wiley–Interscience, New York.
12. J. J. Markam, *Rev. Modern Phys.* **31,** 956 (1959).
13. R. H. Bartram, *in* "Tunable Solid State Lasers," Springer Series in Optical Sciences, Springer-Verlag, New York/Berlin.
14. I. Ya. Gerlovin, *Opt. Spektrosk.* **43,** 530 (1977).
15. D. L. Wood, J. Ferguson, K. Knox, and J. F. Dillon, Jr., *J. Chem. Phys.* **39,** 890 1963).